Coordination Polymers

DOI: 10.1002/anie.200702390

Two-Step Adsorption/Desorption on a Jungle-Gym-Type Porous Coordination Polymer**

Kazuhiro Uemura, Yukari Yamasaki, Yuki Komagawa, Kazuhiro Tanaka, and Hidetoshi Kita*

Porous coordination polymers have attracted the attention of chemists,[1] who have an interest in developing nanometer-sized pores that provide novel guest adsorption properties, such as a highly selective adsorption,[2] a threshold pressure for inclusion,[3,4] and hysteresis isotherms.[4] The characteristic adsorption features found in porous coordination polymers are mainly attributed to the flexibility of the framework, where local bond lengths and angles shift or change during guest insertion to accommodate to their sizes and shapes, thereby resulting in pore deformation.[5] Several flexible coordination polymers[3] that exhibit a threshold pressure (P_{th}) for starting guest inclusion have been reported; for example, 2D square-grid-type $[\{Cu(BF_4)_2(4,4'\text{-bipyridine})_2\}_n]$[3g] and 1D chain-type $[\{Rh_2(benzoate)_4(2\text{-ethylpyrazine})\}_n]$[3h] were found to adsorb CO_2 with a sharp uptake which begins at the pressure P_{th}. From a thermodynamic point of view, P_{th} is recognized as the equilibrium pressure between the initial (closed form) and final (open form) states.[3c,f] However, the adsorption mechanisms that have been reported to date for the stepwise isotherms of several host–guest systems[6] are still difficult to understand. Herein, we report unambiguous two-step adsorption/desorption isotherms on $[\{Zn_2(1,4\text{-bdc})_2(dabco)\}_n]$ (**1**, where 1,4-bdc = 1,4-benzenedicarboxylate and dabco = 1,4-diazabicyclo-[2.2.2]octane)—the discussion being based on a thermal analysis that gives the key for clarifying the stepwise adsorption mechanism.

Compound **1** has a jungle-gym-type structure,[7] in which a 2D square grid composed of dinuclear Zn_2 units is bridged by dabco molecules to extend the 2D layers into a 3D structure, thus affording wide open channels (with an area of 7.5 × 7.5 Å^2), which are large enough to allow the passage of small gas molecules.[7b] In spite of its fully connected 3D structure, compound **1** has enough flexibility around the coordination and single bonds to produce three different crystalline forms.[8] Not only gas molecules but also solvents can be adsorbed on **1**. Figure 1 shows the adsorption/desorption isotherms of propan-2-ol ("isopropanol", IPA) on compound **1** at 308 K. The adsorption isotherm shows a sharp increase at low relative pressures (up to point A where $P/P_0 < 0.05$) and then assumes the plateau form of a type I isotherm. After reaching $P_{th,ad}$ (at $P/P_0 = 0.19$), the curve exhibits another sharp increase and finally attains a saturated level (point B, ca. 160 mL(STP) g^{-1}) at which $[\{[Zn_2(1,4\text{-bdc})_2(dabco)]\cdot 4.5\,IPA\}_n]$ (that is, **1**⊃4.5 IPA) is produced. The desorption isotherm does not retrace the adsorption one; instead, it shows an abrupt decrease at $P_{th,de}$ (where $P/P_0 = 0.12$) to reach point A. This hysteresis profile between the adsorption and desorption isotherms was reproducible. Desorption analysis by means of thermal gravimetry also exhibited a two-step profile in which 1.5 IPA molecules/pore were initially desorbed, followed by the desorption of further three IPA molecules/pore (see Figure S5a of the Supporting Information). This characteristic adsorption/desorption behavior—with hysteresis—is caused by the intermediate state $\{[\{Zn_2(1,4\text{-bdc})_2(dabco)\}\cdot 3IPA]_n\}$ (represented by **1**⊃3 IPA) between **1** and **1**⊃4.5 IPA.

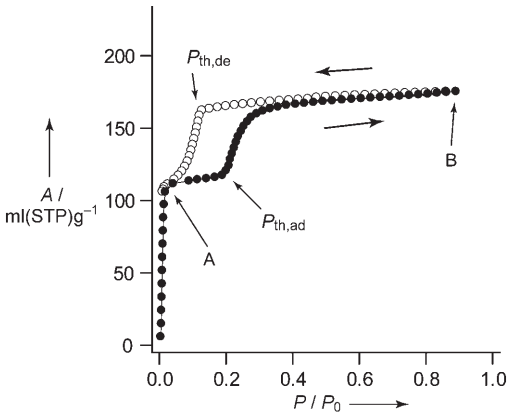

Figure 1. Isotherm of the vapor adsorption (ad, ●) and desorption (de, ○) of propan-2-ol on **1** (at 308 K) over the relative-pressure range from 0 to 0.9 (P_0 is the saturated vapor pressure of propan-2-ol at 308 K, that is, 10.623 kPa). STP = standard temperature and pressure.

The structure of **1**⊃4.5 IPA was determined by means of single-crystal X-ray diffraction (Figure 2). As shown in Figure 2a, the 1,4-bdc ligands that link the Zn_2 paddle-wheel units are linear, thereby forming a perfect 2D square grid linked by disordered dabco pillars. The overall 3D structure is maintained, and the bond lengths and angles around the Zn_2 paddle wheel are similar to those in compound **1**.[7b] The most interesting feature is the position of the adsorbed IPA: Two IPA molecules are coupled by two hydrogen bonds (O–O = 2.65 Å) and remain located among the 1,4-bdc ligands (Figure 2b). These strong pairings induce

[*] Dr. K. Uemura, Y. Yamasaki, Y. Komagawa, Dr. K. Tanaka, Prof. Dr. H. Kita
Environmental Science and Engineering
Graduate School of Science and Engineering
Yamaguchi University, Tokiwadai 2-16-1
Ube-shi, Yamaguchi 755-8611 (Japan)
Fax: (+81) 836-85-9601
E-mail: kazu-u@yamaguchi-u.ac.jp

[**] This work was supported by the Grants-in-Aid for Scientific Research (Young Scientist (B) No. 19750048) and the Kao Foundation for Arts and Sciences.

Supporting information for this article is available on the WWW under http://www.angewandte.org or from the author.

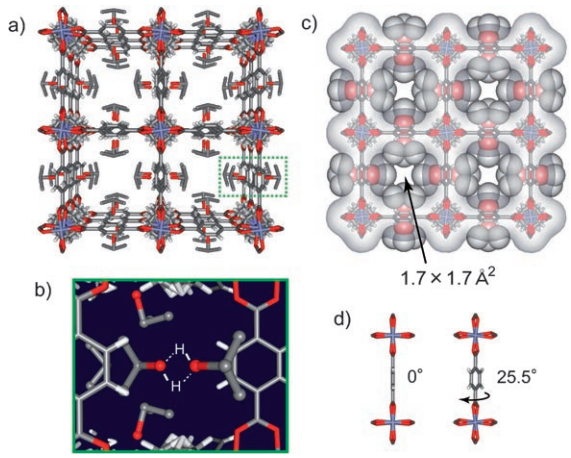

Figure 2. a) Crystal structure of $\{[\{Zn_2(1,4\text{-bdc})_2(dabco)\}\cdot 4.5\,IPA]_n\}$ (**1**⊃4.5 IPA) along the *c* axis. b) Space-filling representation of **1**⊃4.5 IPA along the *c* axis, where open spaces (with an area of 1.7×1.7 Å^2) are filled with highly disordered propan-2-ol molecules. c) Amplified view of the green dotted square in (a) showing propan-2-ol molecules coupled by means of two hydrogen bonds. c) Inclination of the benzene rings without (left, **1**) and with guests (right, **1**⊃4.5 IPA).

a second pore (213 Å^3, 1.7×1.7 Å^2)—surrounded by hydrophobic alkyl moieties of IPA (Figure 2c)—in which other IPA molecules (0.5 molecule/pore) are included with high disorder. Since the methyl moieties of IPA are close to the benzene rings [with C(methyl)·····C(benzene) = 3.75 Å], the dihedral angles of the benzene rings are inclined (25.5°) relative to the initial angle (Figure 2d).

Figure 3 shows the X-ray powder diffraction spectrum (XRPD) of compounds **1**, **1′**, **1**⊃3 IPA, and **1**⊃4.5 IPA. Powdered samples of **1′** and the intermediate state **1**⊃3 IPA were successfully obtained by interrupting the adsorption measurements at points B and C of Figure 3 (left). The peak positions of compound **1′** are shifted to somewhat higher 2θ values than those of compound **1**, which indicates that the framework is slightly shrunk in the **1**→**1′** process. Compound **1**⊃3 IPA has a different crystalline form from that of compounds **1**, **1′**, and **1**⊃4.5 IPA, which shows that the adsorption/desorption of IPA on **1** is accompanied by structural changes. The reflections of **1**⊃3 IPA were indexed with an orthorhombic cell by using the indexing program DICVOL91;[9,10] the reflections of this compound are similar to those of **1**⊃2 C_6H_6.[7b] The overall framework connectivity in **1**⊃2 C_6H_6 remains the same, but the Zn_2 paddle wheels and 1,4-bdc linkers form a 2D rhombic grid.[7b] To compare the three crystalline forms (namely, **1**, **1**⊃3 IPA, and **1**⊃4.5 IPA), the parameters *k*, *l*, *m*, and *n* are defined according to Figure 4 (and the corresponding values are summarized in Table 1).

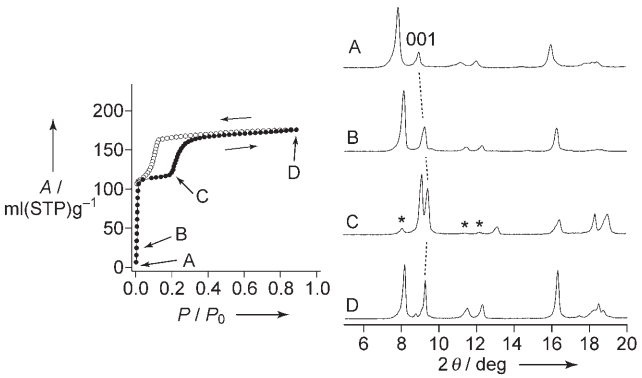

Figure 3. Isotherm (left) of the vapor adsorption (●) and desorption (○) of propan-2-ol on **1** (at 308 K), and XRPD patterns (right) of A) **1**, B) **1′**, C) **1**⊃3 IPA, and D) **1**⊃4.5 IPA at room temperature. Samples **1′** and **1**⊃3 IPA for the XRPD measurements were obtained by interrupting the propan-2-ol adsorption measurements at points B and C, respectively. In C, the asterisks indicate the **1**⊃4.5 IPA phase, where further propan-2-ol adsorption proceeds via the **1**⊃3 IPA phase.

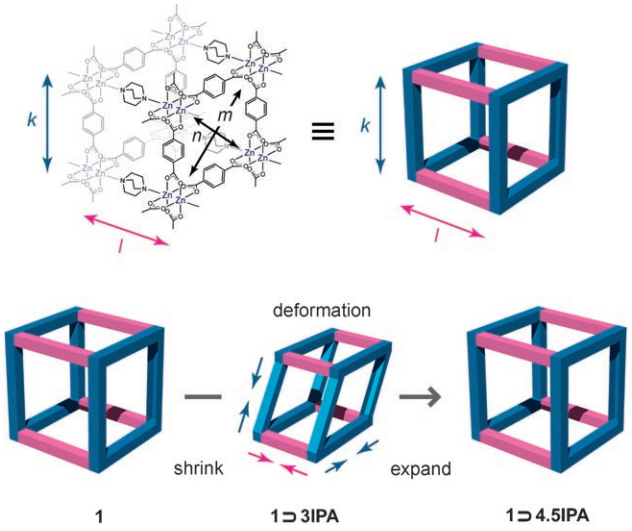

Figure 4. Framework **1** during the adsorption of propan-2-ol. The parameters *k*, *l*, *m*, and *n* are estimated from the unit-cell parameters obtained from the X-ray analysis.

Compound **1**⊃3 IPA shows a shrinkage of the pores and a deformation of the perfect 2D grid (which turns into a rhombic 2D grid) upon inclusion of three IPA molecules/pore; this shrinkage can be attributed to the smaller values of *k* and *l* for this compound relative to those of compounds **1** and **1**⊃4.5 IPA. The [001] reflection of **1**⊃3 IPA, which corresponds to the Zn–Zn–dabco length, unambiguously shifts to higher 2θ values, thus indicating that this compound is shrinking. The parameters of V_{box}, which is defined as the volume of a rectangle surrounded by eight Zn_2 corners, were determined to be 1147 (for **1**), 904 (for **1**⊃3 IPA), and 1135 Å^3 (for **1**⊃4.5 IPA).

Considering both the results of the X-ray analysis and the adsorption isotherms, the mechanism of IPA adsorption on **1**

Table 1: Parameters *k*, *l*, *m*, *n*, and V_{box} of **1**, **1**⊃3 IPA, and **1**⊃4.5 IPA.

	1	**1**⊃3 IPA	**1**⊃4.5 IPA
k [Å]	10.9288(15)	10.058(10)	10.880(1)
l [Å]	9.6084(12)	9.316(4)	9.5846(19)
m [Å]	15.456(2)	16.112(6)	15.387(2)
n [Å]	15.456(2)	12.044(19)	15.387(2)
V_{box} [Å^3]	1147	904	1135

can be explained as follows: In the process $\mathbf{1}+3\,\mathrm{IPA}\rightarrow \mathbf{1}\supset 3\,\mathrm{IPA}$, three IPA molecules/pore are loaded, and specific interactions between these IPA molecules and the framework cause a shrinkage of the framework until point A (see Figure 1). This shrinkage induces a slowing down of the adsorption kinetics. A further increase in the adsorption pressure after point $P_{th,ad}$ leads to a reopening of the total porosity and a complete pore filling ($\mathbf{1}\supset 3\,\mathrm{IPA}+1.5\,\mathrm{IPA}\rightarrow \mathbf{1}\supset 4.5\,\mathrm{IPA}$), which is accompanied by IPA rearrangements. In contrast, another porous coordination polymer, namely, $[\{Cu_2(pzdc)_2(pyz)\}_n]$ (**CPL-1**, where pzdc = pyrazine-2,3-dicarboxylate and pyz = pyrazine), adsorbs acetylene via an expanding-intermediate framework (as shown by in situ synchrotron powder diffraction experiments),[11] and this is—to the best of our knowledge—the first example of the detection of a metastable state in the adsorption process. Interestingly, in the case of compound **1**, the IPA molecules are adsorbed via a shrunken-intermediate framework, which induces further adsorption by means of the breathing mechanism.

Thermal analysis provides additional detailed information about the adsorption process. Figure 5 shows the dependence of P_{th} on the temperature: lowering the measurement temperature causes a decrease of both threshold pressures (with the desorption-threshold pressure remaining lower, see Table 2). The second adsorption begins almost vertically at a definite pressure (namely, $P_{th,ad}$) that should permit guest inclusion.[3] In a similar way, a predominant desorption occurs at pressures lower than the adsorption-threshold pressure, which is denoted as "threshold desorption pressure" ($P_{th,de}$). Since P_{th} can be regarded as the equilibrium pressure for IPA inclusion, its temperature dependence allows us to evaluate the adsorption enthalpy for the IPA adsorption process based on the Clausius–Clapeyron equation.[3c,f,12] This relation can be applied to the threshold pressures of both the adsorption and the desorption processes, thereby showing a linear relationship between the logarithm of the threshold pressure and the reciprocal of the measurement temperature. The adsorption enthalpy for the second IPA adsorption (that is, for the process $\mathbf{1}\supset 3\,\mathrm{IPA}+1.5\,\mathrm{IPA}\rightarrow\mathbf{1}\supset 4.5\,\mathrm{IPA}$) is $\Delta H_{ad,2}=-81.6\,\mathrm{kJ\,mol^{-1}}$.[13] In contrast, the adsorption enthalpy for the first process (namely, $\mathbf{1}+3\,\mathrm{IPA}\rightarrow\mathbf{1}\supset 3\,\mathrm{IPA}$), which was estimated from differential scanning calorimetry data by considering the vaporization enthalpy of IPA, is $\Delta H_{ad,1}=-69.6\,\mathrm{kJ\,mol^{-1}}$.[14] The larger $\Delta H_{ad,2}$ value can be attributed to the formation of two-hydrogen-bonded IPA pairs (see Figure 2b), which exactly balances the endothermic framework transformation in $\mathbf{1}\supset 3\,\mathrm{IPA}+1.5\,\mathrm{IPA}\rightarrow\mathbf{1}\supset 4.5\,\mathrm{IPA}$.

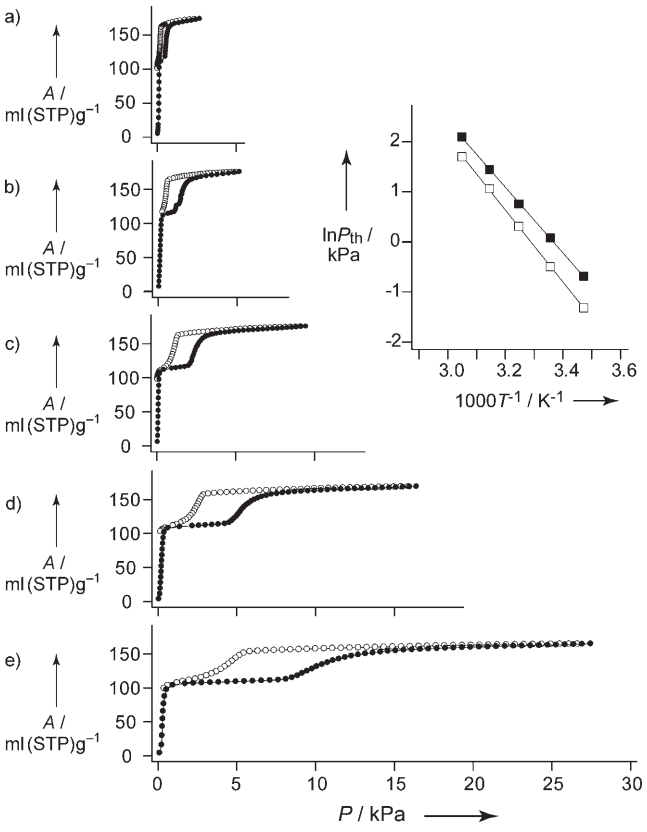

Figure 5. Left: Isotherms of the vapor adsorption (●) and desorption (○) of propan-2-ol on **1** at a) 288, b) 298, c) 308, d) 318, and e) 328 K. P_0 is the saturated vapor pressure of propan-2-ol, namely 3.158 kPa (at 288 K), 5.930 kPa (at 298 K), 10.623 kPa (at 308 K), 18.244 kPa (at 318 K), and 30.171 kPa (328 K). Right: Plots of $\ln P_{th,ad}$ (■) and $\ln P_{th,de}$ (□) against T^{-1}.

Table 2: Temperature dependence of $P_{th,ad}$ and $P_{th,de}$.

T [K]	$P_{th,ad}$ [kPa]	$P_{th,de}$ [kPa]
288	0.51	0.27
298	1.08	0.61
308	2.13	1.36
318	4.24	2.89
328	8.12	5.44

In summary, we have highlighted a stepwise isotherm for the adsorption of IPA on compound **1**, thereby demonstrating that the steps are caused by the shrunk intermediate state $\mathbf{1}\supset 3\,\mathrm{IPA}$. Similar stepwise adsorption isotherms were also confirmed in the case of high-silica zeolites with permanent porosities (such as ZSM-5) as a result of H_2O-cluster formation.[15] Our results imply that the steps observed in the adsorption isotherms of porous coordination polymers are induced by several metastable states—in this case a shrinking framework—which result from the flexibility of the framework. Currently, an attempt to apply thermal analysis to other adsorption systems that include compound **1** is in progress.

Experimental Section

Sample Preparation: The compound $[\{[Zn_2(1,4\text{-bdc})_2(dabco)]\cdot 4\,DMF\cdot{}^1\!/_2 H_2O\}_n]$ ($\mathbf{1}\supset 4\,DMF\cdot{}^1\!/_2 H_2O$) was prepared according to the reported procedure.[7b] The apohost $[\{Zn_2(1,4\text{-bdc})_2(dabco)\}_n]$ (**1**) was obtained by drying in vacuum at 393 K (for 16 h); the formation was checked by means of XRPD measurements. $[\{[Zn_2(1,4\text{-bdc})_2(dabco)]\cdot 4.5\,IPA\}_n]$ ($\mathbf{1}\supset 4.5\,\mathrm{IPA}$) was prepared by exposing **1** to propan-2-ol for 4 days, while $[\{[Zn_2(1,4\text{-bdc})_2(dabco)]\cdot 3\,IPA\}_n]$ ($\mathbf{1}\supset 3\,\mathrm{IPA}$) was obtained by interrupting the propan-2-ol adsorption measurement on **1**.

X-ray Structure Determination of $\mathbf{1}\supset 4.5\,\mathrm{IPA}$: Single crystals of $\mathbf{1}\supset 4.5\,\mathrm{IPA}$ were mounted on a glass fiber and coated with epoxy resin.

The X-ray data collection was carried out by using a Rigaku Mercury diffractometer with graphite monochromated $Mo_{K\alpha}$ radiation ($\lambda = 0.71073$ Å) and a two-dimensional charge-coupled detector (CCD). The sizes of the unit cells were determined from reflections collected on the setting angles of six frames by changing ω by 0.5° for each frame. Two different χ settings were used. Intensity data were collected with a ω scan width of 0.5°. Empirical absorption correction was performed for all the data using REQABA.[16] The structures were solved by the direct method with subsequent difference-Fourier syntheses and a refinement with the SHELXTL (version 5.1) software package.[17] The non-hydrogen atoms were refined anisotropically and all hydrogen atoms were placed in the ideal positions. Crystal data of **1**⊃4.5 IPA: $C_{17}H_{10}NO_6Zn$, $M_w = 389.63$, tetragonal, space group *P*4/*nbm*, $a = 15.387(2)$, $c = 9.5846(19)$ Å, $V = 2269.4(6)$ Å^3, $Z = 4$, $\rho_{calc} = 1.140$ g cm^{-3}, $\mu(Mo_{K\alpha}) = 1.106$ mm^{-1}, *F*-(000) = 788, crystal size = 0.30 × 0.30 × 0.20 mm^3, $T = 223$ K, λ-($Mo_{K\alpha}$) = 0.71073 Å, $\theta_{min-max} = 3.4$–27.5°, total data = 15003, unique data = 1377, $R_{int} = 0.0606$, observed data [$I > 2\sigma(I)$] = 894, $R = 0.0688$, $R_w = 0.2007$, GOF = 1.171. The C4 and C5 atoms were refined with the disorder relationship, the C4 atom being isotropically refined. The propan-2-ol molecule, which includes the O2, C6, and C7 atoms, was isotropically refined under rigid conditions. CCDC 639940 (**1**⊃4.5 IPA) contains the supplementary crystallographic data for this paper. These data can be obtained free of charge from the Cambridge Crystallographic Data Centre via www.ccdc.cam.ac.uk/data_request/cif.

Thermal gravimetry (TG) was carried out with a Rigaku Instrument TG8120 in a helium flow (100 mL min^{-1}). Differential scanning calorimetry (DSC) was carried out with a Rigaku Instrument TG8230 in a nitrogen flow (70 mL min^{-1}), and the heats of desorption were calibrated by melting high-purity indium, lead, and antimony. IR spectra were recorded on a JASCO FT/IR-610 spectrophotometer (with samples prepared with KBr). X-ray powder diffraction (XRPD) data were collected on a Rigaku RINT-2200YS diffractometer with CuKα radiation.

Received: June 1, 2007
Revised: June 16, 2007
Published online: July 30, 2007

Keywords: adsorption · host–guest systems · polymers · X-ray diffraction · zinc

[1] a) O. M. Yaghi, M. O'Keeffe, N. W. Ockwig, H. K. Chae, M. Eddaoudi, J. Kim, *Nature* **2003**, *423*, 705; b) S. Kitagawa, R. Kitaura, S.-i. Noro, *Angew. Chem.* **2004**, *116*, 2388; *Angew. Chem. Int. Ed.* **2004**, *43*, 2334; c) G. Férey, C. Mellot-Draznieks, C. Serre, F. Millange, *Acc. Chem. Res.* **2005**, *38*, 217; d) S. Kitagawa, K. Uemura, *Chem. Soc. Rev.* **2005**, *34*, 109.

[2] For examples, see: a) S. K. Makinen, N. J. Melcer, M. Parvez, G. K. H. Shimizu, *Chem. Eur. J.* **2001**, *7*, 5176; b) K. Uemura, S. Kitagawa, M. Kondo, K. Fukui, R. Kitaura, H.-C. Chang, T. Mizutani, *Chem. Eur. J.* **2002**, *8*, 3586; c) S. Uchida, N. Mizuno, *J. Am. Chem. Soc.* **2004**, *126*, 1602; d) T. K. Maji, K. Uemura, H.-C. Chang, R. Matsuda, S. Kitagawa, *Angew. Chem.* **2004**, *116*, 3331; *Angew. Chem. Int. Ed.* **2004**, *43*, 3269.

[3] a) D. Li, K. Kaneko, *Chem. Phys. Lett.* **2001**, *335*, 50; b) H. Noguchi, A. Kondoh, Y. Hattori, H. Kanoh, H. Kajiro, K. Kaneko, *J. Phys. Chem. B* **2005**, *109*, 13851; c) K. Uemura, S. Kitagawa, K. Fukui, K. Saito, *J. Am. Chem. Soc.* **2004**, *126*, 3817; d) T. K. Maji, G. Mostafa, R. Matsuda, S. Kitagawa, *J. Am. Chem. Soc.* **2005**, *127*, 17152; e) S. Takamizawa, T. Saito, T. Akatsuka, E.-i. Nakata, *Inorg. Chem.* **2005**, *44*, 1421; f) K. Uemura, S. Kitagawa, K. Saito, K. Fukui, K. Matsumoto, *J. Therm. Anal. Calorim.* **2005**, *81*, 529; g) A. Kondo, H. Noguchi, S. Ohnishi, H. Kajiro, A. Tohdoh, Y. Hattori, W.-C. Xu, H. Tanaka, H. Kanoh, K. Kaneko, *Nano Lett.* **2006**, *6*, 2581; h) S. Takamizawa, K. Kojima, T. Akatsuka, *Inorg. Chem.* **2006**, *45*, 4580.

[4] a) R. Kitaura, K. Fujimoto, S.-i. Noro, M. Kondo, S. Kitagawa, *Angew. Chem.* **2002**, *114*, 141; *Angew. Chem. Int. Ed.* **2002**, *41*, 133; b) K. Seki, *Phys. Chem. Chem. Phys.* **2002**, *4*, 1968; c) X. Zhao, B. Xiao, A. J. Fletcher, K. M. Thomas, D. Bradshaw, M. J. Rosseinsky, *Science* **2004**, *306*, 1012.

[5] For examples, see: a) H. J. Choi, T. S. Lee, M. P. Suh, *Angew. Chem.* **1999**, *111*, 1490; *Angew. Chem. Int. Ed.* **1999**, *38*, 1405; b) D. V. Soldatov, J. A. Ripmeester, S. I. Shergina, I. E. Sokolov, A. S. Zanina, S. A. Gromilov, Y. A. Dyadin, *J. Am. Chem. Soc.* **1999**, *121*, 4179; c) C. J. Kepert, M. J. Rosseinsky, *Chem. Commun.* **1999**, 375; d) K. Biradha, Y. Hongo, M. Fujita, *Angew. Chem.* **2002**, *114*, 3545; *Angew. Chem. Int. Ed.* **2002**, *41*, 3395; e) E. Y. Lee, S. Y. Jang, M. P. Suh, *J. Am. Chem. Soc.* **2005**, *127*, 6374; f) C.-L. Chen, A. M. Goforth, M. D. Smith, C.-Y. Su, H.-C. zur Loye, *Angew. Chem.* **2005**, *117*, 6831; *Angew. Chem. Int. Ed.* **2005**, *44*, 6673; g) K. Uemura, K. Saito, S. Kitagawa, H. Kita, *J. Am. Chem. Soc.* **2006**, *128*, 16122.

[6] a) A. J. Fletcher, E. J. Cussen, T. J. Prior, M. J. Rosseinsky, C. J. Kepert, K. M. Thomas, *J. Am. Chem. Soc.* **2001**, *123*, 10001; b) S. Bourrelly, P. L. Llewellyn, C. Serre, F. Millange, T. Loiseau, G. Férey, *J. Am. Chem. Soc.* **2005**, *127*, 13519; c) K. Yamada, H. Tanaka, S. Yagishita, K. Adachi, T. Uemura, S. Kitagawa, S. Kawata, *Inorg. Chem.* **2006**, *45*, 4322.

[7] a) K. Seki, W. Mori, *J. Phys. Chem. B* **2002**, *106*, 1380; b) D. N. Dybtsev, H. Chun, K. Kim, *Angew. Chem.* **2004**, *116*, 5143; *Angew. Chem. Int. Ed.* **2004**, *43*, 5033; c) H. Chun, D. N. Dybtsev, H. Kim, K. Kim, *Chem. Eur. J.* **2005**, *11*, 3521; d) S. Horike, R. Matsuda, D. Tanaka, S. Matsubara, M. Mizuno, K. Endo, S. Kitagawa, *Angew. Chem.* **2006**, *118*, 7384; *Angew. Chem. Int. Ed.* **2006**, *45*, 7226.

[8] Compound **1** is composed of dinuclear Zn_2 units (with a paddle-wheel structure), which are bridged by 1,4-bdc to form 2D square-grid {[Zn_2(1,4-bdc)$_2$]$_n$}. The axial sites of the Zn_2 paddle wheels are occupied by dabco molecules, which act as pillars to extend the 2D layers into a 3D structure. Three kinds of crystal structures, namely, **1**⊃4 DMF·$^1/_2$ H_2O, **1**, and **1**⊃2 C_6H_6 (depending on the guest molecules), have been reported.

[9] A. Boultif, D. J. Louer, *J. Appl. Crystallogr.* **1991**, *24*, 987–993. Orthorhombic, $a = 12.044(19)$ Å, $b = 16.112(6)$ Å, $c = 9.316(4)$ Å, $V = 1808$ Å^3.

[10] The reflections of **1′** were indexed with an orthorhombic cell; orthorhombic, $a = 10.91(2)$ Å, $b = 10.73(2)$ Å, $c = 9.57(5)$ Å, $V = 1122$ Å^3.

[11] Y. Kubota, M. Takata, R. Matsuda, R. Kitaura, S. Kitagawa, T. C. Kobayashi, *Angew. Chem.* **2006**, *118*, 5054; *Angew. Chem. Int. Ed.* **2006**, *45*, 4932.

[12] $d(\ln P)/d(T^{-1}) = \Delta H_{ad}/R$ for the adsorption process, where R and ΔH_{ad} denote the gas constant and the adsorption enthalpy of the guest, respectively.

[13] The corresponding desorption enthalpy is estimated as 89.3 kJ mol^{-1}.

[14] The vaporization enthalpy of IPA is 45.39 kJ mol^{-1}. D. R. Lide, *CRC Handbook of Chemistry and Physics*, *76th ed.*, CRC, Boca Raton, **1995**.

[15] a) D. H. Olson, S. A. Zygmunt, M. K. Erhardt, L. A. Curtiss, L. E. Iton, *Zeolites* **1997**, *18*, 347; b) D. H. Olson, W. O. Haag, W. S. Borghard, *Microporous Mesoporous Mater.* **2000**, *35–36*, 435.

[16] R. A. Jacobson, *REQABA Empirical Absorption Correction*, Version 1.1-03019.98, Molecular Structure Corp., The Woodlands, TX, **1996–1998**.

[17] *SHELXTL Reference Manual*, ver. 5.1, Bruker AXS, Analytical X-Ray Systems, Madison, WI, **1997**.

